Observational Study

Medicine®

OPEN

The application of x-ray, computed tomography, and magnetic resonance imaging on 22 pediatric Langerhans cell histiocytosis patients with long bone involvement

A retrospective analysis

Xiaojun Zhang, MM[a,*], Jing Zhou, MM[b], Xuee Chai, BS[a], Guiling Chen, MM[a], Bin Guo, BS[a], Lei Ni, MM[a], Peng Wu, MM[c]

Abstract

The studies focusing on x-ray, computed tomography (CT), and magnetic resonance imaging (MRI) in pediatric Langerhans cell histiocytosis (LCH) patients were still rare. Therefore, we aimed to evaluate the application of x-ray, CT, and MRI in pediatric LCH patients with long bone involvement.

Total 22 pediatric LCH patients were included in this study. The diagnosis of LCH was confirmed by pathological examination. All patients were followed up for 3 years. X-ray, CT, or MRI was performed and the results were recorded for further analyses.

Among 22 pediatric patients, x-ray (n = 20), CT (n = 18), or MRI (n = 12) were used to scan the lesion on long bones affected by LCH. Femurs (n = 13, 38.24%), tibia (n = 11, 32.35%), humerus (n = 5, 14.71%), and radius (n = 4, 11.76%) were the most frequently affected anatomic sites. Ovoid or round radiolucent lesions, aggressive periosteal reaction, and swelling of surrounding soft tissues were characteristic image of long bones on x-ray, CT, and MRI in pediatric LCH.

Femurs, tibia, humerus, and radius were the most commonly affected long bones of pediatric LCH. The application of x-ray, CT, and MRI on long bones could help with the diagnosis of pediatric LCH.

Abbreviations: CT = computed tomography, LCH = Langerhans cell histiocytosis, MR = magnetic resonance, MRI = magnetic resonance imaging, PET = positron-emission tomography, SD = standard deviations, STIR = short time inversion recovery sequences.

Keywords: computed tomography, magnetic resonance imaging, pediatric langerhans cell histiocytosis, radiological characteristics, x-ray

Highlights

1. Ovoid or round radiolucent lesions, aggressive periosteal reaction were the image features for LCH patients.
2. Swelling of surrounding soft tissues were another image characteristic in LCH patients.
3. Femurs, tibia, humerus, and radius were the most commonly affected long bones of pediatric LCH.
4. X-ray, CT, and MRI could help with the diagnosis of pediatric LCH.

1. Introduction

Langerhans cell histiocytosis (LCH) is characterized by abnormal proliferation of pathological Langerhans cells.[1] In 1953, Lichtenstein discovered and introduced the word of the "histiocytosis X" to describe a group of rare diseases with similar histopathological characteristics, which included Hand-Schüller-Christian syndrome, Letterer-Siwe disease, and eosinophilic granuloma of the bone.[2] Langerhans cell infiltrated multiple organs. Children aging between 1 and 15 years old were most vulnerable to be affected by LCH, while those under 3 years old had the peak incidence. Additionally, the incidence of LCH

Editor: Majid Assadi.

XZ, JZ, and XC should be regard as co-first authors.

The authors declare that they have no competing interests.

[a] Department of Radiology, [b] Department of Radiology, Affiliated Hospital of Nanjing University of Chinese Medicine, [c] Department of Hematology, Children's Hospital of Nanjing Medical University, Nanjing, China.

[*] Correspondence: Xiaojun Zhang, Department of Radiology, Children's Hospital of Nanjing Medical University, No.72 Guangzhou Road, Nanjing 210008, China (e-mail: JuddyZZX8@163.com).

Medicine (2018) 97:17(e0411)

Received: 10 October 2017 / Received in final form: 20 March 2018 / Accepted: 22 March 2018

http://dx.doi.org/10.1097/MD.0000000000010411

was higher in men than the women.[3,4] In 80% of the pediatric LCH cases, bones were mostly affected,[5] especially vertebral bodies, long bones, and mandibles.[6]

The diagnosis of LCH was mainly based on physical examination and tissue biopsy. However, radiological images,[7] including x-ray, computed tomography (CT), and magnetic resonance imaging (MRI), were also recommended in the guideline to diagnose LCH and assess the destruction and necrosis of the bones, the periosteal reaction, and the location and size of soft tissue mass.[8] X-ray examination had its advantages in identifying periosteal reaction and sclerotic margins. MRI was able to find bone destruction and was sensitive in detecting the involvement of the medullary cavity and the soft tissue swelling compared with CT. Moreover, MRI was preferable by pediatric patients because of its non-radioactive character. Nevertheless, although recommended by the guideline, the studies focusing on x-ray, CT, and MRI images of LCH were still rare.[9,10] Clinical doctors still relied on biopsy to make final diagnosis but not based on a good understanding of radiological images. The long bone involvement, which was a quite common affected organ in LCH, was recommended to be assessed by CT and MRI[7] and patients with long bone involvement were always pediatrics under 15 years old.[11]

Furthermore, positron-emission tomography (PET) as a nuclear medicine functional imaging technique, is rapidly evolving in oncology field.[12] Radioactive tracers were used to emit gamma rays after introducing to body on the biologically active molecule for PET scanning. Although PET scanning is non-invasive, body are exposed to ionizing radiation. FDG (2-[fluorine-18]fluoro-2-deoxy-d-glucose) is the widely used tracer for PET, which has an effective radiation dose of 14 mSv.[13] Children are more prone to develop tumor induced by radiation, compared with adults. In this paper, we aimed to investigate the application of x-ray, CT, and MRI of long bone in the diagnosis of pediatric LCH. Therefore, our study evaluated x-ray, CT, and magnetic resonance (MR) images and pathological results of 22 pediatric LCH patients with long bone involvement.

2. Methods

2.1. Participants

From January 2013 to January 2016, the clinical information of 22 pediatric patients with long-bone LCH in Nanjing Children's Hospital was retrospectively analyzed. The inclusion criteria included patients who were diagnosed with LCH by pathological examinations, including H&E staining and immunohistochemical stain, according to the updated guideline[14]; patients underwent x-ray, CT, or MRI examination of the affected long bones; patients under 15 years old. The exclusion criteria included: patients who were diagnosed with LCH but without long bone involvement; patients who had other long bone diseases.

This study was approved by the Ethics Committee of Nanjing Children's Hospital.

2.2. Pathological features

H&E staining and immunohistochemical staining were used to confirm the pathological diagnosis. The diagnosis of LCH in our study was based on positive immunohistochemical staining for S-100 protein and the demonstration of T6 (CD1a) antigenic determinants on the surfaces of lesion cells from biopsy samples.[15]

2.3. Radiological examination

X-ray, CT, or MR images were performed and recorded. CT was performed using Philips Brilliance 64 Slice CT workstation. Thirty minutes before CT scan, 5% chloral hydrate (1 mL/kg) was orally administered to sedate the children when necessary. CT imaging parameters were set as follows: section thickness, 0.625 mm; tube voltage, 120 keV; tube current, 80 mAs, and pitch = 1. All the data were transferred to the workstation via Picture Archiving and Communication System (PACS). The post-processing techniques included multiplanar reconstruction and volume rendering, with a reconstruction interval of 1 to 3 mm. MRI was performed at 1.5 T using a Siemens superconducting MRI scanner. Scan parameters were set as follows: repetition time (TR) 623 ms; 22 ms of echo time (TE), 180° of flip angle, and 3 mm of slice thickness for T1WI; TR 4960 ms, TE 105 ms, flip angle 150°, slice thickness 3.5 mm for T2WI; and TR 3450 ms, TE 89 ms, flip angle 150°, slice thickness 3 mm for short time inversion recovery sequences (STIR). Sagittal STIR, T1WI and T2WI images, coronal STIR images, and transaxial T2WI images were acquired. Two experienced radiologists who were blind to the results of other examinations evaluated the images separately. If the 2 radiologists had different opinions, a third radiologist was invited to review the image data and give a final result. The locations and character of LCH lesion on long bones were recorded for further analyses.

2.4. Treatments

A total of 14 patients underwent curettage and allogeneic bone graft surgery and postoperative chemotherapy, while 8 patients were subjected to chemotherapy. The chemotherapy were administered according to the modified German–Austrian (DAL-HX 83/90) method.[16]

2.5. Follow-up

Participants were followed up for 3 years. Specifically, patients were followed up every 2 months for the first 6 months after surgery and every 3 months during 6 to 12 months. After the first year after surgery, participants were followed up every 6 months for the subsequent 2 years. X-ray, CT, or MRI was performed in follow-up period.

2.6. Outcome evaluation

According to the guidelines for the diagnosis and treatment of LCH for patients under the age of 18 years,[16] 3 degrees of patients' response to treatment were proposed: good response, moderate response, and exacerbation. The response degrees were based on the disappearance of the primary lesion and the appearance of the new lesion. If the primary lesion disappeared and no new lesion was found, then the response was defined as good. If the density of the lesion gradually became even, the bone density increased, the hardening margin appeared around the medullary cavity, and the corresponding cortical bone thickening with a limited trend, the response was moderate. If the lesion did not get smaller or disappear after treatment, or there were new lesions, the response was deteriorative or exacerbated.

Table 1

Localization of long-bone lesions on pediatric Langerhans cell histiocytosis patients.

Injury locations	No. of patients	%
Femur	13	38.24
Tibia	11	32.35
Humerus	5	14.71
Radius	4	11.76
Ulna	1	2.94

2.7. Statistical analysis

The data were analyzed by SPSS software (V22.0, Chicago, IL). All the continuous data were presented as mean ± SD (standard deviations) and categorical data were presented as percentages. The differences between groups were analyzed by *t* test or continuous data and Chi-square test for categorical data. All *P* values were 2-tailed, and $P < .05$ was considered statistically significant.

3. Results

3.1. Participants

Total 22 pediatric patients with long-bone LCH were included in this study, including 14 boys and 8 girls, ranging from 1 to 8 years old, with a median age of 3 years old. The disease course ranged from 1 to 25 months. The clinical manifestations of the 22 LCH children mainly present with local pain or claudication (n = 20), fever lasting for 2 weeks (n = 1), and frontal mass (n = 1).

3.2. Pathological results

Based on HE staining, the lesions of patients were present with gray-red and dark-red bone tissues of hard texture mixed with granulation-like tissue. In this study, the biopsy results of all patients were positive for S-100 protein and CD1a antigen.

3.3. Localization of LCH lesions based on x-ray, CT, and MRI

There were 11 patients (50%) with single long bone lesions, including tibia (4/22, 36.36%), femur (3/22, 27.27%), radius (3/22, 27.27%) and ulna (1/22, 9.09%), and 11 patients (11/22, 50%) who had multiple long bone involvement with a total of 23 lesions, including femur (10 sites), humerus (5 sites, including 1 patient had epiphysis involvement), tibia (7 sites), and radius (1 site). The total lesion sites included the femur (n = 13, 38.24%), tibia (n = 11, 32.35%), humerus (n = 5, 14.71%), radius (n = 4, 11.76%), and ulna (n = 1, 2.94%). Details were available in Table 1. Most lesions affected the diaphysis and metaphysis, while only 1 lesion affected the epiphysis.

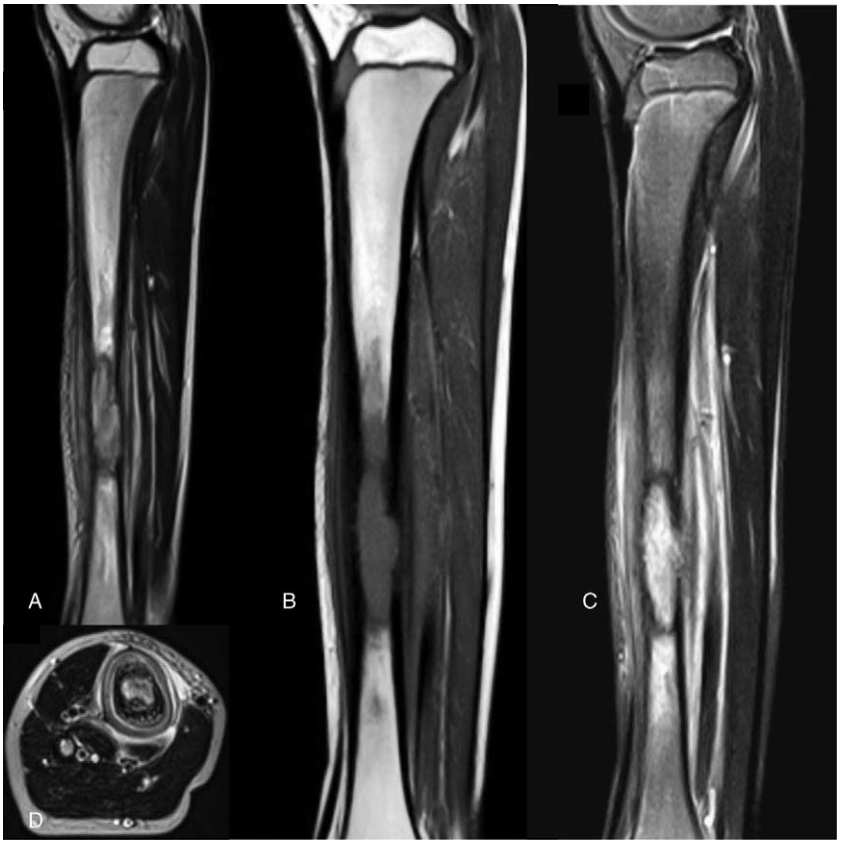

Figure 1. T2WI, T1WI, and STIR MR sequences of the right tibia of an 8-year-old boy with Langerhans cell histiocytosis. The ovoid lesion with isointense and hypointense signals on T1 sequence (A) and hyperintense signals on T2 sequence (B) were detected in the lower 1/3 of the medullary cavity of the right tibia. The lesion had a sclerotic margin, which showed hyperintense signals on STIR sequence (C). There was also a layered periosteal reaction (D). MR = magnetic resonance, STIR = short time inversion recovery sequences.

Figure 2. X-ray (A), CT (B), and MRI STIR sequence (C) of left femur from a 6-year-old boy with Langerhans cell histiocytosis. Destructive oval lesions were observed in the middle left femoral diaphysis on x-ray, CT, and STIR sequence. These lesions were associated with thickly lamellated periosteal reaction and soft tissue swelling. The STIR image showed extensive high intense signal in the medullary cavity: CT (D) and MRI STIR sequence (E) of a 2-year-old boy with Langerhans cell histiocytosis. At the middle of the right tibial diaphysis, lytic bone destruction associated with periosteal reaction and soft tissue mass was observed. CT = computed tomography, MR = magnetic resonance, STIR = short time inversion recovery sequences.

3.4. Features of LCH on X-ray, CT, and MRI

X-ray (n = 20) and CT (n = 18) images indicated thick diaphysis and thin cortical bone. Round or ovoid radiolucent areas suggested osteolytic, cystic, or expansile bone destruction. The lesions were well circumscribed, while marginal sclerosis were observed in 2 patients (9.09%) (Figs. 1 and 2). Other manifestations included soft tissue swelling (n = 21, 95.45%), soft tissue mass (n = 1, 4.55%), and periosteal reaction (n = 19, 86.36%). The cross-sectional scanning of CT (n = 18) could completely show lytic and periosteal reaction and showed the medullary bone destruction (n = 18, 100%) and cortical bone destruction (n = 15, 83.33%) (Table 2). In 1 patient, x-ray showed mild periosteal reaction at the proximal ulnar bone, but CT images found that the bone density was heterogeneously reduced in the medullary cavity with periosteal reaction and soft tissue swelling surrounded. MRI (n = 12) revealed that intramedullary focal lesions with extramedullary soft-tissue, which had low intensity signal on T1 weighted sequence and high intensity signal T2 weighted sequence (n = 12, 100%), were surrounded by ring-shaped or multilayer periosteal reaction (n = 12, 100%). Massive abnormal signals were found in the proximate medullary cavity and they showed high intensity signals on STIR. Other manifestations included cortical bone destruction (n = 12, 100%), soft tissue swelling, and soft tissue mass (Fig. 2, Table 2).

3.5. Follow-up

All the participants were followed up for 3 years to evaluate the prognosis and x-ray, CT, and MRI were examined. The follow-up images revealed more homogeneous density within the lesion, increased bone density, re-appeared medullary cavity, and increased cortical bone thickness. There were 2 patients (2/22, 9.09%) who had good response after treatment (Fig. 3), while 3 patients (3/22, 13.64%) were exacerbated. The other 17 patients had moderated response after treatment.

Table 2

X-ray, CT, and MRI manifestation of long bones of pediatric Langerhans cell histiocytosis patients.

	X-ray		CT		MRI	
Manifestations	**No**	**%**	**No.**	**%**	**No.**	**%**
Lytic	20	100	18	100	0	0
Soft tissue swelling	19	95	17	94.44	11	91.67
Periosteal reaction	17	77.27	18	100	12	100
Expansile	14	70	13	72.22	9	75
Cortical destruction	10	50	15	83.33	12	100
Increased bone density	8	40	0	0	0	0
Soft tissue mass	1	5	1	5.56	1	8.33
Reactive marginal sclerosis	1	5	2	11.11	0	0
Increased intramedullary density	0	0	18	100	0	0
Intramedullary lesion with extramedullary soft-tissue extension	0	0	0	0	12	100

CT = computed tomography; MRI = magnetic resonance imaging.

4. Discussion

LCH is a quite rare, complex, and multifaceted group of disorder. The etiology of LCH was not clearly known.[17] LCH affected 5 persons per 1 million people,[5] and more than half of the cases were diagnosed under 15 years old.[18,19] The clinical presentation of LCH variated. Bones, skin, oral cavity, genitals, lung, and other organs could be affected.[7] Up to 50% of LCH occurred in bones.[19] Biopsy was still a golden standard for the diagnosis of LCH, but radiological measures, including CT and MRI, were also recommended to evaluate LCH and assist in the diagnosis.[20] X-ray was convenient, cheap, and easy to perform in clinical practice. Therefore, we evaluated the application of x-ray, CT, and MRI on 22 pediatric LCH patients with long bone involvement in this study.

The prevalence of LCH in our study was consistent with previous results.[3,4] Moreover, we found that single long-bone LCH lesion mostly localized in tibia (4/22, 36.36%), followed by femur, radius, and ulna, while multiple long-bone LCH lesions frequently localized in femur, followed by tibia, humerus, radius, and ulna orderly. Long-bone LCH primarily affected metaphysis or diaphysis, but not epiphysis.[21] In keeping with that notion, the lesion started from medullary cavity of the long bone and progressed outwards, which led to thinner and damaged cortical bones. Typically, the affected areas are round-shaped or oval-shaped lesions.[2] In the present study, epiphysis involvement was observed only in 1 patient (1/22), which was consistent with the previous opinions. In the case of lesion sites, femurs, tibia, humerus, and radius were the most frequently affected anatomic sites, which was slightly different from the previous report.[22] Bone destruction could be cystic or osteolytic. Occasionally, an expanded cortical shell developed as the lesion grew and destroyed the native bones. The periosteal reaction varied in magnitude, with characteristic multilayer onion-skin or single-layer morphology.[23] The x-ray and CT showed round-shaped or ovoid-shaped, well circumscribed, and radiolucent defects within the medullary cavity. Moreover, the sclerotic margin showed a high density on CT and ring-shaped high density on T2WI. However, mature lesions were rare, with only 2 cases in our study. The periosteal reactions with typical layered or onion-

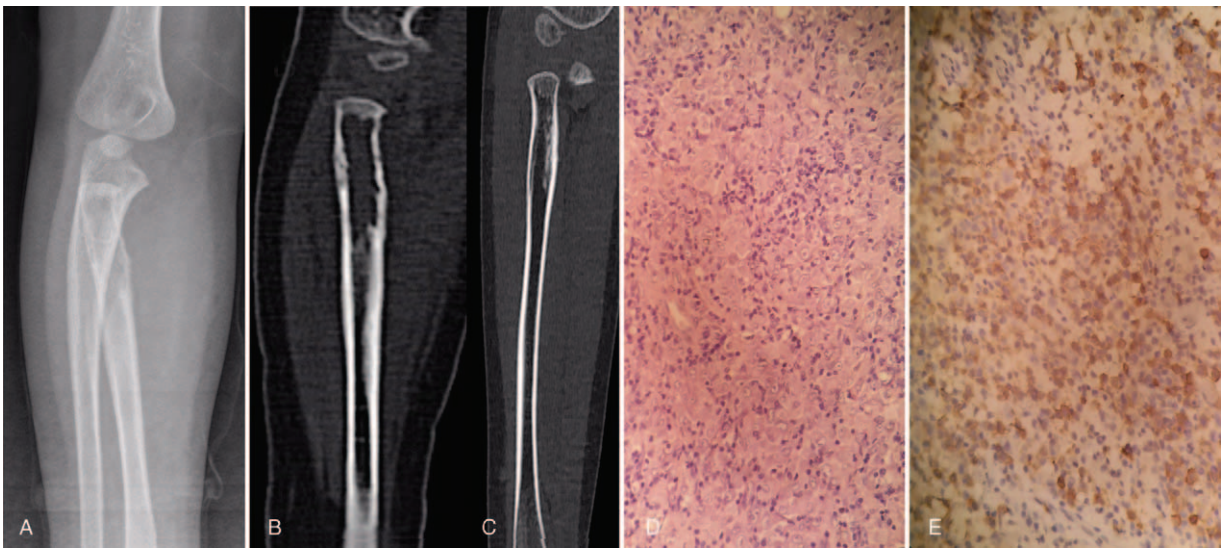

Figure 3. X-ray (A), CT (B and C), pathological (D), and histological (E) images right ulna from a 4-year-old boy with Langerhans cell histiocytosis. Bone destruction associated with mild periosteal reaction on right proximal ulna was observed (A and B). After 25 months of chemotherapy, the bone density of proximal ulna and the cortical bone thickness became normal (C). CT = computed tomography.

skin morphology were frequently observed. Furthermore, most lesions were surrounded by soft tissue edema and only one lesion was surrounded by soft tissue mass.

CT was sensitive to osteolysis, and lamellated periosteal reaction.[24] With the development of CT technology, the current multi-detector CT can perform multi-plane reorganization and observe bone details. Accordingly, CT image of LCH was characterized by increased density of medullary cavity and the destruction of cortical bone, while x-ray showed lytic and periosteal reaction of LCH.

MRI depicted intramedullary lesions with extramedullary soft-tissue components. On the T1WI sequence, the lesions had iso-intensity or low intensity signals while the signal of the lesion was higher than the adjacent muscles. On the T2WI sequence, the lesion showed generally high intensity signals, while some lesion had a lacelike peripheral appearance, which might be due to the difference of growth rates within the cancerous tissue. Moreover, the lesions observed on MRI had a higher resolution ratio than those on CT images, which could be explained by the natural poor sensitivity of CT on edema surrounding bone marrow and soft tissue. The sagittal and coronal plane of MRI typically had characteristic cuffing features, which were caused by eosinophilic granuloma and mononuclear phagocyte infiltration of cortical periosteum.[25]

Several key factors affected the clinical outcome of LCH,[5,7] such as LCH infiltration condition and the involvement of organs. It had been reported that the emergence of marginal sclerosis was an indicator of mature and localized lesions.[26] Patients with LCH might experience spontaneous remission, and the healing of bone lesions gradually occurred through the progression of fibrosis. During the follow-up period of this study, the density of the lesion turned normal, while the overall bone density increased. Later on, the lesion became well circumscribed with the formation of marginal sclerosis. The medullary cavity reappeared and the thickness of affected cortical bone increased, then the lesion was confined. The clinical outcomes of the 22 patients were satisfactory. Two out of the 22 patients experienced complete remission. In the current study, 11 patients who had multiple lesions, did not respond well to the treatment. Generally, patients with single organ involvement, relatively longer disease courses, localized lesions, and those who underwent systematic treatments[27,28] had favorable prognosis.

5. Conclusion

Ovoid or round radiolucent lesions, aggressive periosteal reaction, and swelling of surrounding soft tissues were the main characteristics based on the images of x-ray, CT, and MRI of long bones on pediatric LCH patients. Femurs, tibia, humerus, and radius were the most commonly affected long bones of pediatric LCH. The application of x-ray, CT, and MRI on long bones could help with the diagnosis of pediatric LCH.

Author contributions

Conceptualization: Xiaojun Zhang.
Data curation: Lei Ni.
Formal analysis: Jing Zhou, Lei Ni.
Investigation: Bin Guo.
Methodology: Xuee Chai.
Project administration: Xuee Chai, Guiling Chen.
Software: Guiling Chen.
Supervision: Xuee Chai, Peng Wu.
Validation: Guiling Chen, Bin Guo.
Writing – original draft: Xiaojun Zhang, Jing Zhou.
Writing – review & editing: Peng Wu.

References

[1] Zinn DJ, Chakraborty R, Allen CE. Langerhans cell histiocytosis: emerging insights and clinical implications. Oncology (Williston Park) 2016;30:122–32. 139.
[2] Stull MA, Kransdorf MJ, Devaney KO. Langerhans cell histiocytosis of bone. Radiographics 1992;12:801–23.
[3] Wang J, Wu X, Xi ZJ. Langerhans cell histiocytosis of bone in children: a clinicopathologic study of 108 cases. World J Pediatr 2010;6:255–9.
[4] Vadivelu S, Mangano FT, Miller CR, et al. Multifocal Langerhans cell histiocytosis of the pediatric spine: a case report and literature review. Childs Nerv Syst 2007;23:127–31.
[5] Badalian-Very G, Vergilio JA, Fleming M, et al. Pathogenesis of langerhans cell histiocytosis. Annu Rev Pathol 2013;8:1–20.
[6] Merglová V, Hrušák D, Boudová L, et al. Langerhans cell histiocytosis in childhood - review, symptoms in the oral cavity, differential diagnosis and report of two cases. J Craniomaxillofac Surg 2014;42:93–100.
[7] Dicaprio MR, Roberts TT. Diagnosis and management of Langerhans cell histiocytosis. J Am Acad Orthop Surg 2014;22:643–52.
[8] Harmon CM, Brown N. Langerhans cell histiocytosis: a clinicopathologic review and molecular pathogenetic update. Arch Pathol Lab Med 2015;139:1211–4.
[9] Kilborn TN, Teh J, Goodman TR. Paediatric manifestations of Langerhans cell histiocytosis: a review of the clinical and radiological findings. Clin Radiol 2003;58:269–78.
[10] Hirt HP, Berthold H, Burkhardt A. [Oral manifestations in histiocytosis X. The clinical, radiological and therapeutic aspects]. Schweiz Monatsschr Zahnmed 1991;101:328–38.
[11] Khatami A, Alavi S, Valeshabad AK, et al. Radiologic manifestations of langehans cell histiocytosis in pediatrics. PJR 2010;20:114–20.
[12] Macpsem DLB, Arcp, Fipem, Pd DWT, Fracp PEVM. Positron Emission Tomography. Springer Berlin 2013; 45:481–486.
[13] Kelloff GJ, Hoffman JM, Johnson B, et al. Progress and promise of FDG-PET imaging for cancer patient management and oncologic drug development. Clinical Cancer Research An Official Journal of the American Association for Cancer Research 2005;11:2785–808.
[14] Haupt R, Minkov M, Astigarraga I, et al. Langerhans cell histiocytosis (LCH): guidelines for diagnosis, clinical work-up, and treatment for patients till the age of 18 years. Pediatr Blood Cancer 2013;60:175–84.
[15] Robak T, Kordek R, Robak E, et al. Langerhans cell histiocytosis in a patient with systemic lupus erythematosus: a clonal disease responding to treatment with cladribine, and cyclophosphamide. Leuk Lymphoma 2002;43:2041–6.
[16] Schäfer T, Bauer CP, Beyer K, et al. S3-Guideline on allergy prevention: 2014 update: Guideline of the German Society for Allergology and Clinical Immunology (DGAKI) and the German Society for Pediatric and Adolescent Medicine (DGKJ). Allergo J Int 2014;23:186–99.
[17] Morimoto A, Oh Y, Shioda Y, et al. Recent advances in Langerhans cell histiocytosis. Pediatr Int 2014;56:451–61.
[18] Maria PA, del Prever AB, Pagano M, et al. Langerhans cell histiocytosis: 40 years' experience. J Pediatr Hematol Oncol 2012;34:353–8.
[19] Arkader A, Glotzbecker M, Hosalkar HS, et al. Primary musculoskeletal Langerhans cell histiocytosis in children: an analysis for a 3-decade period. J Pediatr Orthop 2009;29:201–7.
[20] Girschikofsky M, Arico M, Castillo D, et al. Management of adult patients with Langerhans cell histiocytosis: recommendations from an expert panel on behalf of Euro-Histio-Net. Orphanet J Rare Dis 2013;8:72.
[21] Postini AM, Andreacchio A, Boffano M, et al. Langerhans cell histiocytosis of bone in children: a long-term retrospective study. J Pediatr Orthop B 2012;21:457–62.
[22] Hashmi MA, Haque N, Chatterjee A, et al. Langerhans cell histiocytosis of long bones: MR imaging and complete follow up study. J Cancer Res Ther 2012;8:286–8.
[23] Routy B, Hoang J, Gruber J. Pulmonary langerhans cell histiocytosis with lytic bone involvement in an adult smoker: regression following smoking cessation. Case Rep Hematol 2015;2015:201536.
[24] Galyfos G, Karantzikos GA, Kavouras N, et al. Extraosseous ewing sarcoma: diagnosis, prognosis and optimal management. Indian J Surg 2016;78:49–53.
[25] Grosjean F, Nasi S, Schneider P, et al. Dendritic cells cause bone lesions in a new mouse model of histiocytosis. PLoS One 2015;10:e0133917.
[26] Grana N. Langerhans cell histiocytosis. Cancer Control 2014;21:328–34.
[27] Parikh SN, Desai VR, Gupta A, et al. Langerhans cell histiocytosis of the clavicle in a 13-year-old boy. Case Rep Orthop 2014;2014:510287.
[28] Abraham A, Alsultan A, Jeng M, et al. Clofarabine salvage therapy for refractory high-risk langerhans cell histiocytosis. Pediatr Blood Cancer 2013;60:E19–22.